Development of the g-C_3N_4/$BiVO_4$ Microflower Photocatalyst for Photocatalytic Degradation of Amoxicillin and Hydrogen Production

Mohamad Fakhrul Ridhwan Samsudin[1], Arthur Dumas[2], Robabeh Bashiri[3], Norani Muti Mohamed[3],Suriati Sufian[1,3,*]

[1] Chemical Engineering Department, Universiti Teknologi PETRONAS, 32610, Bandar Seri Iskandar, Perak, Malaysia.
[2] École Nationale Supérieure en Génie de Technologies Industrielles (ENSGTI), Université des Pays de l'Adour, Rue Jules Ferry, BP 7511, 64 075 Pau Cedex, France.
[3]Centre of Innovative Nanostructures & Nanodevices (COINN), Universiti Teknologi PETRONAS, 32610, Bandar Seri Iskandar, Perak, Malaysia.

Abstract

A novel g-C_3N_4/$BiVO_4$ microflower photocatalyst was synthesized via a modified hydrothermal method. The physicochemical properties of the g-C_3N_4/$BiVO_4$ microflower photocatalyst were scrutinized via XRD, FESEM and DR-UV-Vis analysis. The performances of the g-C_3N_4/$BiVO_4$ microflower photocatalyst were assessed through the photocatalytic degradation of amoxicillin antibiotic and the photoelectrocatalytic hydrogen production. It was found that the g-C_3N_4/$BiVO_4$ microflower photocatalyst was capable of producing up to 14.35 mmol/h of hydrogen. Meanwhile, 89.5% of amoxicillin antibiotic was successfully degraded within 3 hours under visible-light-irradiation. The profound photocatalytic performances of the g-C_3N_4/$BiVO_4$ microflower photocatalyst were attributed to the intimate contact between both photocatalyst, results in a smooth photocharge carrier separation and migration, evidently from the FESEM analysis. It is anticipated that this work will serve as a breakthrough in the photocatalytic applications via designing microflower type photocatalysts with remarkable performance.

Keywords: bismuth vanadate, graphitic carbon nitride, photocatalysis, degradation, hydrogen

Article Info

Received 24th October 2019
Accepted 16th March 2020
Published 1st April 2020
*Corresponding author: Suriati Sufian; e-mail: suriati@utp.edu.my

ISSN: 1823-7010, eISSN: 2600-7444

Introduction

Since the discovery of the TiO_2 photocatalyst for photocatalytic application by Honda and Fujishima in 1970 [1], the exploration of the photocatalyst materials has significantly increased for the past decades. Photocatalytic technology has been denoted as an alternative approach to replace the non-green fossil fuel system in order to mitigate global environmental and energy security issues. Nevertheless, the conventional photocatalyst materials are greatly suffered from the fast recombination rate of the electron-hole pair and wide bandgap energy, consequently limits the practical application of this technology [2]. Thus, it is imperative to design and develop novel and highly functionalized photocatalyst materials in order to enhance their performance for the requirements of clean hydrogen energy and environmental remediation technology. Among various photocatalyst, bismuth vanadate ($BiVO_4$) with a bandgap energy of 2.4 eV has been widely explored as a visible-light-driven photocatalyst [3]. Nevertheless, the activity of this material is hampered due to several factors such as excessive charge recombination and poor photocharge transfer [4]. Various strategies have been devoted to mitigate the abovementioned limitations including nanoarchitectures, facet-engineering and coupling with other semiconductor materials to form the heterostructure system [2, 3].

The formation of the heterostructure system is considered as a novel approach to mitigate the aforementioned problems facing by the single photocatalyst. There are two factors that need to be considered while designing the composite heterostructure systems which are (i) the appropriate band edge location which can promote the photocharge separation and migration at the junction interfaces and (ii) excellent photocharge transfer property [4]. Interestingly, graphitic carbon nitride (g-C_3N_4) photocatalyst has an appealing band edge location for the formation of the heterostructure system with $BiVO_4$. The matching band edge position between $BiVO_4$ and g-C_3N_4 allows the electron to smoothly migrate towards the adjacent photocatalyst and limits the possibility of the recombination rate to occur. Moreover, the optical property of the g-C_3N_4 photocatalyst which possesses medium bandgap energy (~2.7 eV) signifies the capability of this material to absorb the visible-light energy [5].

Herein, the photocatalytic activity of the g-C_3N_4/$BiVO_4$ microflower photocatalyst prepared via a modified hydrothermal method was evaluated in photoelectrocatalytic hydrogen production and degradation of amoxicillin antibiotic. To the best authors' knowledge, studies on the benefits of g-C_3N_4/$BiVO_4$ microflower photocatalyst in both applications are hardly been found in any literature.

Materials and Methods

Preparation of Photocatalysts

The conventional $BiVO_4$ photocatalyst was prepared as reported in the previous publication [4]. Generally, a respective amount of vanadium oxide, V_2O_5 (assay at 99.0%) and bismuth (II) oxide, Bi_2O_3 (assay at 99.9%) were thoroughly mixed in an aqueous HNO_3 solution. The suspension was stirred for 4 days. Finally, the suspension was centrifuged, washed and dried in an oven at 90 °C.

The $BiVO_4$ microflower photocatalyst was prepared using a hydrothermal method. Initially, 3 mmol of $Bi(NO_3)_3.5H_2O$ (assay at 98.0%) and 3 mmol of NH_4VO_3 (assay at 99.0%) were separately suspended in 30 mL of 2 M HNO_3 solution and denoted as solution A and B,

respectively. Then, solutions A and B were mixed and stirred for one hour prior to the pH adjustment using ethylenediamine (pH = 1.96). Afterward, the mixing solution was sonicated for 30 minutes. The solution was poured into a 100 mL Teflon-lined stainless-steel autoclave. The temperature was set at 120 °C and kept for 5 hours. Finally, the yellowish solution was centrifuged, washed and dried in an oven at 90 °C.

The g-C_3N_4 photocatalyst was prepared according to the literature [6]. Generally, 10 g of urea powder was transferred into a quartz silica crucible with lid and calcined in a furnace. The furnace was set as follows: temperature: 500 °C, heating rate: 5 °C/min and duration: 2 hours. Lastly, the sample was naturally cooled before collected and used without further treatment.

The g-C_3N_4/$BiVO_4$ microflower sample was prepared using a wet-impregnation method. Initially, a respective amount of g-C_3N_4 was weighed and mixed with 1 g of $BiVO_4$ photocatalyst. Then, 50 mL of deionized water was added to the mixture and the solution was continuously stirred for 1 hour before heating at 70 °C. After the solution become slurry, the paste was dried in an oven at 90 °C. Finally, the sample was regrinding in order to produce fine particles of the composite sample.

The crystalline phase of the product was examined using X-ray diffraction (XRD; Model: X'Pert^3 powder and Empyrean, PANalytical). A scanning electron microscope (SEM, Zeiss Supra 55VP) with a magnification of 10Kx was used to identify the morphology of the modified photocatalyst. The optical properties of the modified photocatalysts were examined using DR-UV-Vis Spectrophotometer (Cary 100s) to obtain the energy threshold of the structure.

Photocatalytic Evaluation Performance

The photocatalytic degradation activity was examined via the degradation of amoxicillin (10 mg/L). Generally, 0.1 g sample and 100 mL of the wastewater were added into a glass reactor and left stirring for 1 hour. This step is important for establishing the adsorption-desorption equilibrium. Afterward, the solution was irradiated with a 500 W halogen lamp for 3 hours. Finally, the aliquots sample was analyzed using a UV-Vis spectrophotometer (UV-1800, Shimadzu) at a specific wavelength of 228 nm. Meanwhile, the details of the photocatalytic hydrogen production performance have been reported in the previous publication [7]. The photocatalytic degradation of amoxicillin and photoelectrocatalytic hydrogen production was performed separately.

Result and Discussion

The crystallographic properties of the as-developed photocatalysts were examined via XRD measurement as depicted in Figure 1. Generally, the pure $BiVO_4$ photocatalyst shows splitting peaks located at 18.2,18.9. 29.5 32.7 and 48.5° of 2θ corresponded to the (110), (011), (121), (400) and (202) crystal facet as shown in Figure 1 (a). These diffraction peaks matched well with the monoclinic-scheelite of $BiVO_4$ (JCPDS card no. 14 – 0688) [7]. Additionally, the strongest peak located at 24.6° of 2θ corresponded to the (200) crystal facet. However, this peak coincided well with the tetragonal structure of $BiVO_4$ (JCPDS card no. 14 – 0133) [8]. Thus, it can be said that the as-developed $BiVO_4$ composed of two crystal structures, namely monoclinic-scheelite and tetragonal like structure. Meanwhile, the pure g-C_3N_4 was composed of two diffraction peaks located at 14.2 and 28.4° of 2θ which belongs to the (100) and (002) crystal facets [9].

Figure 1 (b) illustrates the XRD patterns of the as-developed composite g-C_3N_4/$BiVO_4$ microflower photocatalyst. It can be seen that all of the footprints belong to the $BiVO_4$ photocatalyst either the tetragonal or monoclinic-scheelite structure as well as the g-C_3N_4 photocatalyst were found in the XRD analysis, signifying the successful formation of the composite g-C_3N_4/$BiVO_4$ microflower photocatalyst via a wet-impregnation method. Interestingly, the (100) crystal facet of g-C_3N_4 was hardly been visible in the composite XRD analysis. This was presumably due to the simultaneous decrease in planar size and denser stacking of the g-C_3N_4 layers. No extra peaks corresponded to the impurities were detected except the peaks belongs to the $BiVO_4$ and g-C_3N_4 structure.

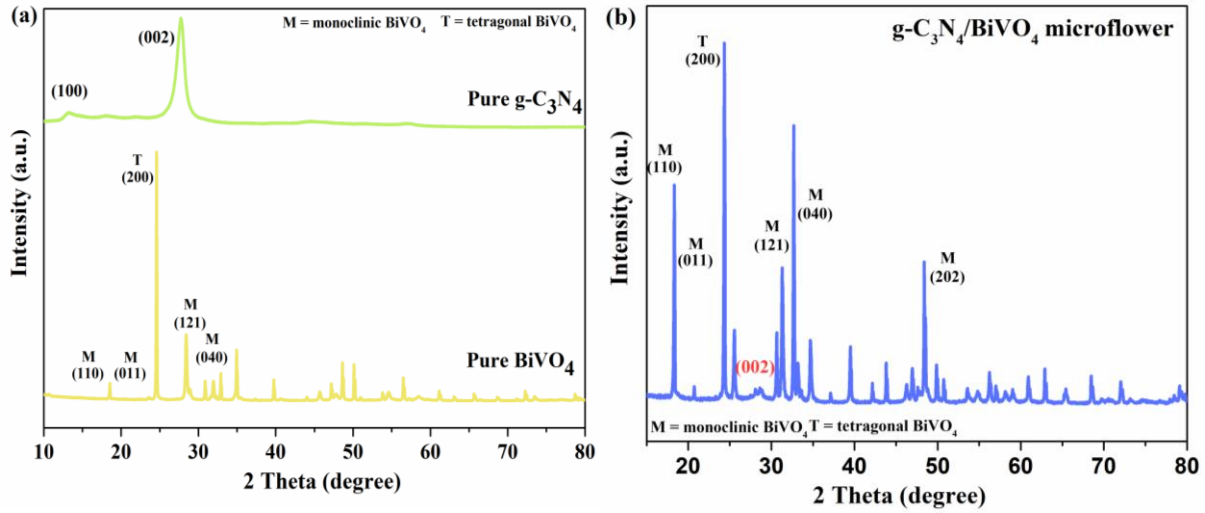

Figure 1: XRD analysis for (a) pure photocatalyst and (b) g-C_3N_4/$BiVO_4$ microflower photocatalyst.

The morphological structures of the samples were shown in Figure 2. Typically, the g-C_3N_4 sample was made up of a crumple sheet-like structure while the conventional $BiVO_4$ prepared via a solid-liquid state reaction was made up of cuboid-decahedral shape like structure [10]. Furthermore, the $BiVO_4$ prepared via a hydrothermal method possesses a microflower-like structure. Similarly, the composite g-C_3N_4/$BiVO_4$ photocatalyst composed of microflower-like structure corresponded to the $BiVO_4$ particle and the small crumple sheet-like structure was attributed to the g-C_3N_4 particles. It can be seen that the g-C_3N_4 particles were intimately attached while randomly distributed on the $BiVO_4$ structures within the g-C_3N_4/$BiVO_4$ microflower sample. The intimate contact between g-C_3N_4 and $BiVO_4$ particles in the heterostructure g-C_3N_4/$BiVO_4$ microflower sample is important as it will facilitate the movement and migration of electron-hole pair between the adjacent photocatalyst, results in better photocatalytic activities [11,12].

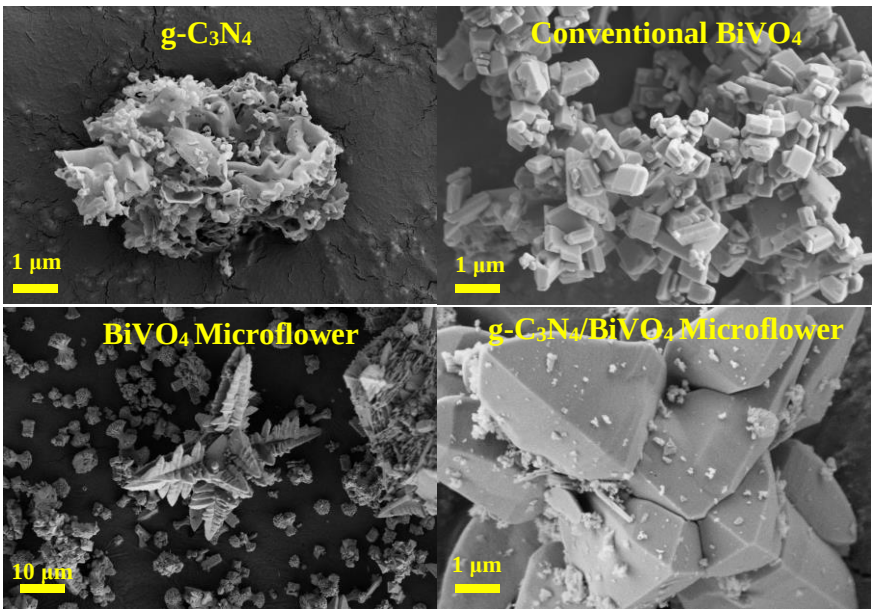

Figure 2: FESEM images of the as-developed photocatalysts.

Table 1 summarizes the bandgap energy which was calculated from the Tauc plot analysis. The conventional $BiVO_4$ possesses bandgap energy of 2.44 eV while the bandgap energy for the $BiVO_4$ microflower was slightly narrower (2.42 eV). Meanwhile, the g-C_3N_4 photocatalyst has medium bandgap energy around 2.88 eV. Upon construction of the g-C_3N_4/$BiVO_4$ microflower photocatalyst heterostructure system, the bandgap energy was found to be 2.72 eV. The calculated bandgap energy highlights that the as-developed photocatalysts possess the absorption capacities within the visible-light range in which it can utilize up to 48% of the total solar light energy, results in better photocatalytic and photoelectrocatalytic performances.

Table 1: Bandgap energy calculated from the Tauc plot analysis.

Sample	Bandgap Energy (eV)
g-C_3N_4	2.88
Conventional $BiVO_4$	2.44
$BiVO_4$ Microflower	2.42
g-C_3N_4/$BiVO_4$ Microflower	2.72

The performance of the as-developed photocatalysts for the amoxicillin degradation was illustrated in

Figure *3* (a). The photocatalytic degradation reaction for amoxicillin was performed under visible-light illumination for 3 hours. It was found that the conventional $BiVO_4$, $BiVO_4$ microflower and g-C_3N_4 photocatalysts were only capable of degrading up to 35.6, 51.3 and 59.4 % of amoxicillin. On the other hand, the composite g-C_3N_4/$BiVO_4$ microflower sample shows the highest performance in the photocatalytic degradation of amoxicillin in comparison to the other samples. Gratifyingly, a similar trend of photoelectrocatalytic performance was observed when all of the photocatalyst samples were evaluated for photoelectrocatalytic hydrogen production. The composite g-C_3N_4/$BiVO_4$ photocatalyst attained the highest hydrogen production of 14.35 mmol/h followed by g-C_3N_4 (6.94 mmol/h), $BiVO_4$ microflower (4.17 mmol/h) and conventional $BiVO_4$ (2.31 mmol/h) as shown in **Figure 3 (b)**.

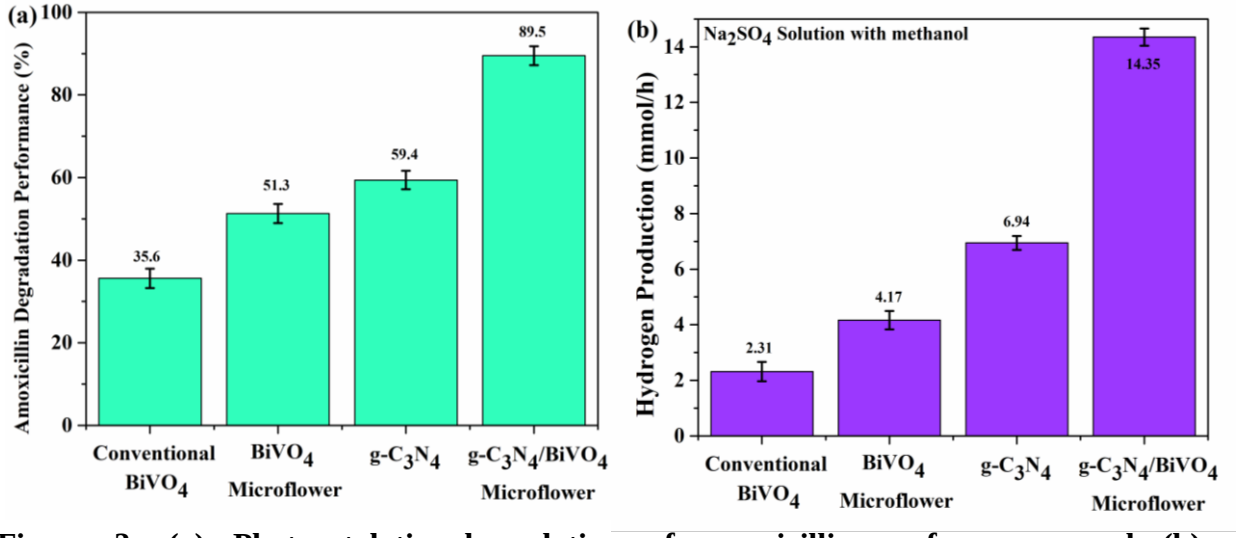

Figure 3: (a) Photocatalytic degradation of amoxicillin performance and (b) photoelectrocatalytic hydrogen production via as-developed photocatalysts under visible-light-irradiation.

The obtained data for both photocatalytic and photoelectrocatalytic performances portray that the pure $BiVO_4$ and g-C_3N_4 exhibit the lowest performance which stemming from the fast recombination of the photocharge carrier, consequently hinder the performance of the pure sample. Nevertheless, the g-C_3N_4/$BiVO_4$ microflower photocatalyst shows a profound performance for both applications. The intimate contact among particles within the g-C_3N_4/$BiVO_4$ microflower photocatalyst and the enhanced optical properties, evidently from FESEM and bandgap energy analysis, respectively allows the photocharge carrier to be smoothly separated and migrated and thus minimizing the possibility of the photocharge carrier recombination, results in better photocatalytic and photoelectrocatalytic activity.

Conclusion

In summary, a novel composite g-C_3N_4/$BiVO_4$ microflower photocatalyst was successfully synthesized and evaluated for photocatalytic degradation of amoxicillin antibiotic and photoelectrocatalytic hydrogen production under visible-light-irradiation. The remarkable photocatalytic activities monitored for the g-C_3N_4/$BiVO_4$ microflower photocatalyst were attributed to the better particles contact within the heterostructure system and enhanced optical properties which facilitate the movement and migration of the photocharge carrier, results in

hindering the photocharge carrier recombination. This works not only present novel photocatalyst materials to be used in the wastewater treatment application, but also the practicality of the as-developed materials to be used in the hydrogen energy technology.

Acknowledgement

This work was supported by Yayasan Universiti Teknologi PETRONAS (015LC0-138). A special thanks to the Chemical Engineering Department and COINN, Universiti Teknologi PETRONAS for the lab facilities.

Author Contributions

The writing of the manuscript, experimental work and data analysis were performed by all authors and agree to be accountable for all aspects of the work.

Disclosure of Conflict of Interest

There is not conflict of interest among authors.

Compliance with Ethical Standards

The work is compliant with ethical standards.

Reference

[1] Honda, A., Fujishima, K. (1972). Electrochemical Photolysis of Water at a Semiconductor Electrode. *Nature*. 238, 37–38.

[2] Xu, M., Yang, J., Sun, C., Liu, L., Cui, Y., Liang, B., (2020). Performance enhancement strategies of bi-based photocatalysts: A review on recent progress. *Chemical Engineering Journal.* 389, 124402.

[3] Jia, J., Sun, W., Zhang, Q., Zhang, X., Hu, X., Liu, E., Fan, J., (2020) Inter-plane heterojuctions within 2D/2D $FeSe_2$/g-C_3N_4 nanosheet semiconductors for photocatalytic hydrogen generation. *Applied Catalysis B: Environmental*, 261, 118249.

[4] Samsudin, M.F.R., Sufian, S., Hameed, B.H., (2018). Epigrammatic progress and perspective on the photocatalytic properties of $BiVO_4$-based photocatalyst in photocatalytic water treatment technology: A review, *Journal of Molecular Liquids*, 268, 438–459.

[5] Inagaki, M., Tsumura, T., Kinumoto, T., Toyoda, M. (2019). Graphitic carbon nitrides (g-C_3N_4) with comparative discussion to carbon materials. *Carbon*. 141, 580–607.

[6] Liu, B., Mu, L., Han, X., Zhang, J., Shi, H., (2019). Highly efficient visible-light-driven photocatalytic activity of g-C_3N_4@Ag/$AgVO_3$ composites for dye degradation and bacterial inactivation. *Journal of Photochemistry and Photobiology A: Chemistry*, 380, 111866.

[7] Samsudin, M.F.R., Sufian, S., Mohamed, N.M., Bashiri, R., Wolfe, F., Ramli, R.M., (2018). Enhancement of hydrogen production over screen-printed TiO_2/$BiVO_4$ thin film in the photoelectrochemical cells, *Materials Letters*, 211, 13–16.

[8] Liu, S., Tang, H., Zhou, H., Dai, G., Wang, W. (2017). Photocatalytic perfermance of

sandwich-like $BiVO_4$ sheets by microwave assisted synthesis. *Applied Surface Sciences*. 391, 542–547.

[9] Putri, L.K., Ng, B.-J., Er, C.-C., Ong, W.-J., Chang, W. S., Mohamed, A.R., Chai, S.-P., (2020). Insights on the impact of doping levels in oxygen diped gC_3N_4 and its effects on photocatalytic activity, *Applied Surface Science,* 504, 144427.

[10] Wang, Z., Huang, X., Wang, X. (2019). Recent progresses in the design of $BiVO_4$-based photocatalysts for efficient solar water splitting, *Catalysis Today*, 335, 31–38.

[11] Baral, B., Reddy, K.H., Parida, K.M., (2019). Construction of M-$BiVO_4$/T-$BiVO_4$ isotype heterojunction for enhanced photocatalytic degradation of Norfloxacine and Oxygen evolution reaction, *Journal of Colloid Interface Sciences,* 554, 278–295.

[12] Tan, H.L., Amal, R., Ng, Y.H. (2017). Alternative strategies in improving the photocatalytic and photoelectrochemical activities of visible light-driven $BiVO_4$: a review, *Journal of Materials Chemistry A*, 5, 16498.